Multi-layer masonry bed joint subjected to shear: Analytical modelling

Originally published in:
Construction and Building Materials 205, https://doi.org/10.1016/j.conbuildmat.2019.02.051

Funding acknowledgement:
169119 - Developement of a Soft Layer for Seismic Response Modification of Structural Masonry Walls (SNF)

Multi-layer masonry bed joint subjected to shear: An analytical model

Nebojša Mojsilović*, Miloš Petrović, Božidar Stojadinović

Institute of Structural Engineering, Department of Civil, Environmental and Geomatic Engineering, ETH Zurich, 8093, Switzerland

*Corresponding author. Tel.: +41446333763. *E-mail address:* mojsilovic@ibk.baug.ethz.ch

Abstract

An analytical rheological model capable of describing the loading speed dependent in-plane shear behaviour of a masonry multi-layer bed joint is presented in this paper. Such joints consist of a core soft layer protected by two thin extruded elastomer membranes, which in turn are placed in a bed mortar joint. The extruded elastomer membranes are employed to prevent and/or limit the deterioration of the core soft layer during the cyclic action observed in previous investigations. Joint behaviour is assumed to be linear elastic-perfectly viscoplastic and has been captured by a uniaxial model consisting of three elements: an elastic spring connected in series with the frictional slider and a dashpot (viscous damper). The rheological model is characterized by three material parameters that have been assessed from several series of monotonic and static-cyclic tests on small masonry specimens (triplets). In addition to these three parameters, the contraction of the thickness of multi-layer bed joint due to pre-compression has been considered too. Although model parameters are determined for the multi-layer bed joint with a rubber granulate core soft layer, the parameter space can be extended to the other types of core soft layer once the appropriate test data becomes available.

Keywords

Analytical model, elastic-viscoplastic behaviour, extruded elastomer, loading-speed, multi-layer bed joint, rubber granulate, sliding, unreinforced masonry.

1. Introduction and previous investigation

In Swiss construction practice, different types of deformable layers, i.e. soft layers, are placed at the bottom of unreinforced masonry (URM) walls. The materials used for soft layers are bitumen, cork, polyvinylchloride and different types of rubber (usually extruded elastomer and rubber granulate). The main purpose of such layers is to act as damp-proof course (DPC) and/or sound insulation. Furthermore, soft layers are used to adjust short- or long-term differential movements between the walls and the floors above and beneath them. Thus, these soft layers are not intended for seismic loading. However, these layers are capable of considerably modifying the seismic response of masonry walls and structures. The research project underlying this paper is exploring the possibilities to take advantage of such behaviour.

Most of the previously conducted research concentrated on the assessment and study of the behaviour of different types of soft layers subjected to static, static-cyclic and dynamic loading. Usually, small specimens (triplets) have been tested under different pre-compression loads. Thereby, the shear response parameters and the overall performance of joints with soft layers were assessed. Shear tests on the URM elements [1–10] indicate that the presence of a soft layer in the horizontal mortar bed joint can considerably alter the mechanical characteristics of such a bed joint by forming a sliding plane that could have a beneficial influence on the seismic response of URM walls. Findings from the experiments on masonry wallettes with rubber granulate and elastomer soft layers confirmed this, see Mojsilović et al. [11], Vögeli et al. [12] and Petrović et al. [13]. During these tests, considerable damage of rubber granulate soft layers (caused by the cyclic motion) was observed. However, the elastomer layers exhibited significantly higher durability. In order to improve the durability, i.e. reduce the deterioration caused by cyclic loading and the overall behaviour of the joints with soft layers, a novel multi-layer bed joint has been recently introduced, see Mojsilović et al. [14]. This joint consists of a core soft layer shielded by two elastomer layers. This soft multi-layer is placed in the middle of the mortar bed joint, see Figure 1. The materials used for the core soft layer were rubber granulate, cork, cork-rubber granulate, bitumen and PVC-based membranes. The findings from several series of monotonic and static-cyclic displacement0controlled tests performed on masonry

triplets with a multi-layer bed joint (Mojsilović et al. [14]) showed that such joints (albeit, with adequate material properties) could change the typical brittle shear response of masonry into a quasi-ductile one with a remarkably larger deformation capacity.

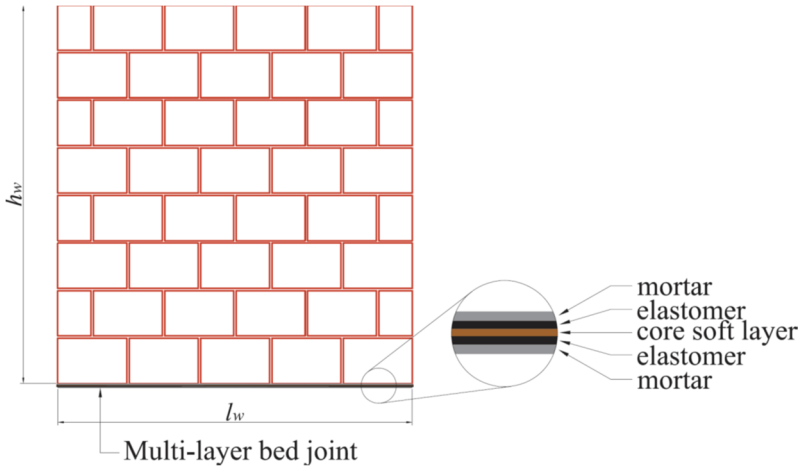

Fig. 1. The multi-layer bed joint at the bottom of the masonry wall

In order to further investigate the behaviour and influence of a multi-layer bed joint in masonry walls, a series of static-cyclic tests on full-scale URM walls has been conducted, see Petrović et al. [15]. It was shown that in masonry structures with multi-layer bed joints a considerable amount of energy can be dissipated, which leads to enhanced seismic performance of such structures. This conclusion is justified from the observed hysteretic behaviour. In addition, it was found that the overall behaviour of masonry with a multi-layer bed joint depends strongly on the loading speed. Most notably, the friction coefficient and thus the shear strength of such bed joints are affected by increasing loading speed. Trajkovski et al. [5] tested masonry triplets with bitumen- and polyester-based DPCs soft layers placed in bed joints and reported similar findings: they found that the loading speed influenced the shear response characteristics. Additionally, Vögeli et al. [12] reported that the friction coefficient is also dependent on the normal pressure (pre-compression) acting at the sliding interface. Totoev and Simundic [6] investigated the pseudo-viscosity of the joints containing DPC, i.e. dependence of the joint response on different strain rates. For this purpose, they performed monotonic tests on DPC membrane (bitumen-coated aluminium and embossed polythene) slip joints placed at the interface between concrete and masonry. Considering all this, it can be concluded that the loading speed and

pre-compression are the most important parameters for an accurate behaviour assessment of masonry multi-layer bed joints during sliding.

A relatively small amount of research data is available on the analytical modelling of the behaviour of masonry with soft layers incorporated in bed joints subjected to static-cyclic shear. However, a considerable amount of data on modelling the behaviour of (mostly rubber-like) materials used in multi-layer bed joints can be found in the literature. The referenced research focused mostly on the non-masonry materials. Thereby, special attention was paid to the non-cohesive interfaces. The reviewed publications concentrated on the investigation of the sliding friction in general [16-19] and on the friction between the elastomer and rough surfaces, e.g. [20-21], in particular. The latter reinforced the findings concerning the loading speeds applied in the current investigation: the friction coefficient increases with increasing loading speed and with decreasing normal pressure applied to the sliding interface. As shown in [14], the friction coefficient increases following, approximately, an exponential law as the loading speed increases. After reaching a maximum value for a particular loading speed, the relationship exhibits a plateau and the friction coefficient remains more or less constant. The dependency of the friction coefficient on loading speed can be described using a bounded monotonically increasing function, which requires that both the minimum and the maximum values of the friction coefficient and one additional fitting parameter be defined, see Mojsilović [14]. The extremal values of the friction coefficient are obtained from tests. More general models on the behaviour of elastic-viscoplastic materials that are appropriate for the modelling of the materials under investigation can be found in the structural mechanics literature, e.g. Ibrahimbegović [22] and de Souza Neto et al. [23].

An analytical rheological model of the loading speed-dependent in-plane shear behaviour of the masonry multi-layer bed joint will be presented in the second section of the paper. The third section presents the results from a series of monotonic in-plane shear and relaxation test performed on masonry triplets with a rubber granulate core soft layer. These results, together with those from the static-cyclic shear tests on masonry triplets with a rubber granulate core soft layer in multi-layer bed joints presented in [14], allow one to determine the model parameters. In the fourth section, the

97 analytical model is calibrated based on the experimental data obtained from our own tests, and its
98 behaviour is discussed. Finally, the last section provides a set of conclusions and gives
99 recommendations for the future research.

100 **2. Analytical model**

101 The shear load-deformation behaviour of a multi-layer bed joint will be as assumed linear elastic-
102 perfectly viscoplastic. Such behaviour can be captured by a uniaxial model consisting of three
103 elements: an elastic spring connected in series with a frictional slider and a dashpot (viscous damper),
104 see Figure 2. Thereby the elastic spring is characterized by the shear modulus of the multi-layer bed
105 joint, G_{ml}, the dashpot by the loading speed sensitive viscosity parameter with the dimension time, ζ,
106 and the frictional slider by the elastic shear stress limit, i.e. sliding resistance, τ_y.

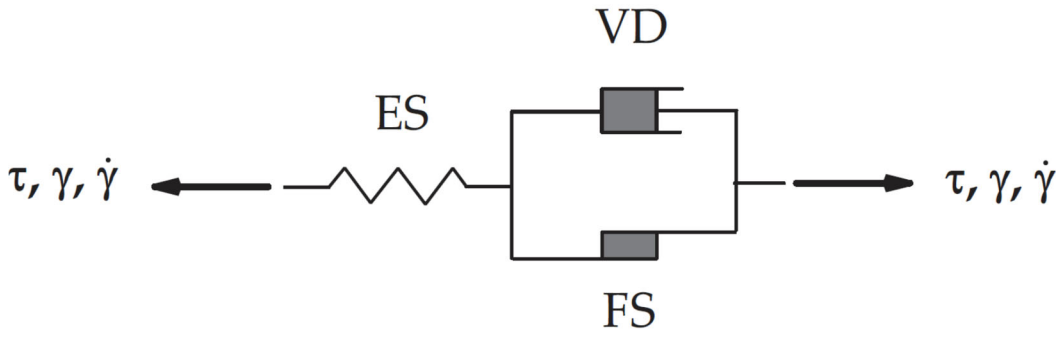

107

108 Fig. 2. The rheological model of a multi-layer bed joint

109 The mechanical behaviour of the model is determined by the following set of equations. A total shear
110 strain, γ, consists of an elastic (recoverable) and a viscoplastic (permanent) component, γ^{el} and γ^{vp},
111 respectively:

112 $$\gamma = \gamma^{el} + \gamma^{vp}. \tag{1}$$

113 The elastic stress-strain relationship reads:

114 $$\tau = G_{ml} \cdot \gamma^{el} \tag{2}$$

115 and the yield function is given by:

116 $$\Phi\left(\tau, \tau_y\right) = |\tau| - \tau_y. \tag{3}$$

Finally, the viscoplastic flow rule reads:

$$\dot{\gamma}^{vp} = \lambda \cdot \frac{\partial \Phi}{\partial \tau} = \lambda \cdot \operatorname{sign}(\tau), \text{ where } \lambda = \begin{cases} \frac{1}{\zeta} \cdot \left[\frac{|\tau|}{\tau_y} - 1 \right] & \text{if } \Phi(\tau, \tau_y) > 0 \\ 0 & \text{if } \Phi(\tau, \tau_y) \le 0 \end{cases} \tag{4}$$

Note that λ is an explicitly given function capable of modelling the dependence of the viscoplastic strain speed on the stress level. Looking at the positive shear stress and strain (for the sake of simplicity) and considering Eq. (1) one obtains for the strain rate

$$\dot{\gamma} = \dot{\gamma}^{el} + \dot{\gamma}^{vp}. \tag{5}$$

Further by considering Eqs. (2) and (4) one obtains

$$\dot{\gamma} = \frac{\dot{\tau}}{G_{ml}} + \frac{1}{\zeta} \cdot \left(\frac{\tau}{\tau_y} - 1 \right) \tag{6}$$

and the relation between stress and strain rates, which is

$$\dot{\tau} + \frac{G_{ml}}{\zeta \cdot \tau_y} \cdot \tau = \frac{G_{ml}}{\zeta} + G_{ml} \cdot \dot{\gamma}. \tag{7}$$

Applying standard methods for solving first-order ordinary linear differential equations, Eq. (7) can be integrated. Note that, according to the model assumption on the elastic-perfectly viscoplastic behaviour of the multi-layer bed joint, the shear yield stress (elastic limit) τ_y is considered as independent of the loading speed. Further, assuming the shear strain speed to be constant and starting from the solution of the differential Eq. (7)

$$\tau(t) = C_1 \cdot e^{-\frac{G_{ml}}{\tau_y \cdot \zeta} \cdot t} + \tau_y \cdot (1 + \zeta \cdot \dot{\gamma}) \tag{8}$$

and substituting $t = \gamma / \dot{\gamma}$, one obtains

$$\tau(\gamma, \dot{\gamma}) = C_1 \cdot e^{-\frac{G_{ml}}{\tau_y \cdot \zeta} \cdot \frac{\gamma}{\dot{\gamma}}} + \tau_y \cdot (1 + \zeta \cdot \dot{\gamma}). \tag{9}$$

With known (force) boundary condition, $\tau(\gamma = \gamma_y) = \tau_y$, the integration constant C_1 can be determined:

136 $$C_1 = -\tau_y \cdot \dot{\gamma} \cdot \zeta \cdot e^{\frac{G_{ml}}{\tau_y \cdot \zeta} \cdot \frac{\gamma_y}{\dot{\gamma}}} \,. \tag{10}$$

137 Finally, the (loading speed dependent) shear stress-shear strain relationship can be written in the
138 following form

139 $$\tau\left(\gamma, \dot{\gamma}\right) = \tau_y \cdot \left[1 + \dot{\gamma} \cdot \zeta \cdot \left(1 - e^{-G_{ml} \cdot \frac{\gamma - \gamma_y}{\tau_y \cdot \zeta \cdot \dot{\gamma}}}\right)\right]. \tag{11}$$

140 This relationship is shown in Fig. 3 for different values of loading speed, together with the limits
141 $\dot{\gamma} \vee \zeta \to 0$ (denoting an infinitely small loading speed or a non-viscous material) and $\dot{\gamma} \vee \zeta \to \infty$
142 (denoting an infinitely large loading speed or an infinitely viscous material).

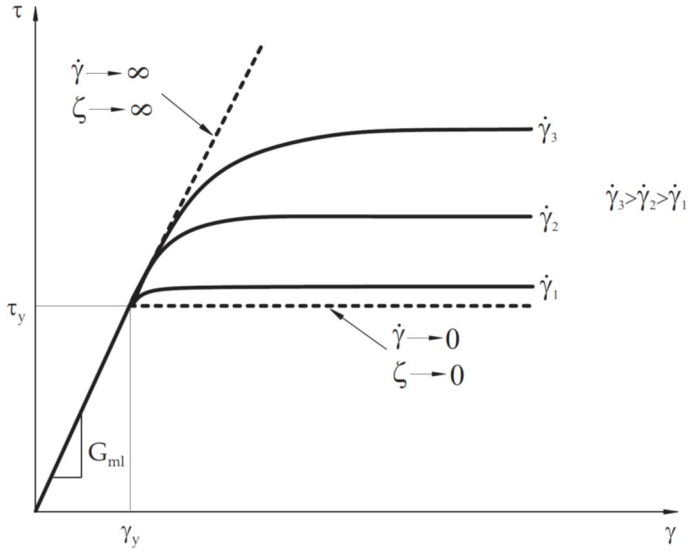

143

144 Fig. 3. Shear stress-shear strain relationship of the rheological model for different values of the
145 loading speed

146 Since the multi-layer bed joint represents a localized zone of intense shearing with constant thickness
147 t_{ml}, the shear strain γ and shear strain rate $\dot{\gamma}$ can be related to the slip in the multi-layer bed joint d
148 and the slip rate $\dot{d}$, respectively, see Oberender and Puzrin [24]. Thus, in addition to the three
149 previously defined parameters of the rheological model, the contraction of the thickness of multi-layer
150 bed joint due to pre-compression, Δt_{ml}, has to be considered too. Thus

151 $$d = \gamma \cdot \left(t_{ml} - \Delta t_{ml}\right) \text{ and } \dot{d} = \dot{\gamma} \cdot \left(t_{ml} - \Delta t_{ml}\right). \tag{12}$$

This allows one to formulate the shear stress-shear deformation (slip) relationship:

$$\tau\left(d,\dot{d}\right)=\tau_y\cdot\left[1+\frac{\dot{d}}{t_{ml}-\Delta t_{ml}}\cdot\zeta\cdot\left(1-e^{-\frac{G_{ml}}{\tau_y\cdot\zeta}\cdot\frac{d-d_y}{\dot{d}}}\right)\right]. \tag{13}$$

As can be seen from Eq. (13), with known thickness of the multi-layer bed joint, one needs four parameters, i.e. τ_y, G_{ml}, ζ, and Δt_{ml} to define the shear stress dependence on the loading speed and the displacement (slip).

Two of four previously-mentioned parameters that describe the deformation of the multi-layer bed joint when subjected to pre-compression and the shear load, i.e. shear modulus, G_{ml}, and the contraction of the thickness of the multi-layer bed joint, Δt_{ml}, have been determined from displacement controlled in-plane monotonic shear tests on masonry triplets with a rubber granulate core soft layer in multi-layer bed joints. In order to assess the values of the third parameter, τ_y, shear relaxation tests were conducted: after reaching the maximum shear force, the relative displacement (slip) in the bed joint has been kept constant in the following and the force relaxation has been recorded. In the Section 3 the results from these tests will be presented and discussed. Finally, in order to determine the remaining model parameter, ζ, while taking into account the elastic (initial) shear stiffness degradation due to cyclic loading, data on the shear capacity from the series of static-cyclic shear tests on masonry triplets with multi-layer bed joints, [14], were used.

3. Experimental investigation

This section presents and discusses the findings obtained by performing a series of monotonic in-plane shear and relaxation tests on masonry triplets with a rubber granulate core soft layer in a multi-layer bed joint. The testing campaign and results have been presented and discussed in detail in Petrović [25]. Here, only the details needed for the current presentation will be given.

3.1. Test programme and masonry materials

Multi-layer bed joints were assembled using a 3 mm thick rubber granulate core layer placed between two 2.2 mm thick protective elastomer layers. Typical Swiss perforated clay blocks, with nominal

dimensions of 290x150x190 mm and a void area of 42% and standard cement mortar were used to construct the triplets, cf. Fig. 4. The thickness of the multi-layer bed joint without the mortar layers was 7.4 mm. The cement mortar used did not allow for mortar layers thinner than about 5 mm, thus resulting in total thickness of the joint of 17.4 mm. The average compressive strength of the perforated block, determined according to the European standard EN 772-1 [26] amounted to 31.5 MPa with a standard deviation of 2.38 MPa. The average compressive strength of the cement mortar was determined according to the European standard EN 1015-11 [27]. Two sets of mortar specimens, which were stored in the climatic chamber and in the open air in the laboratory, were tested. The obtained strengths were 14.84 MPa with a standard deviation of 0.52 MPa, and 6.68 MPa with a standard deviation of 0.43 MPa, respectively.

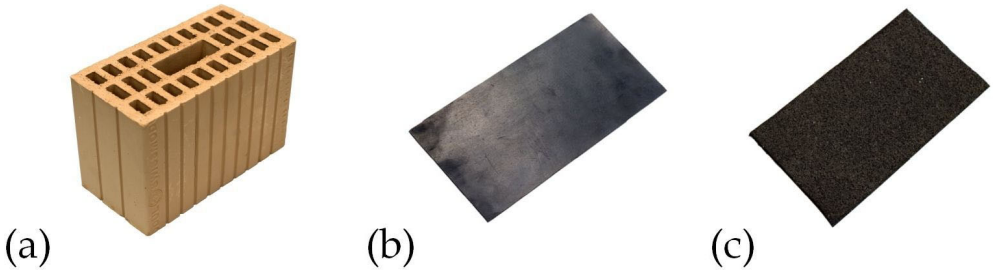

Fig. 4. Masonry materials: a) perforated clay block; b) extruded elastomer; c) rubber granulate

Specimens were organized into three series according to the designated level of pre-compression, σ_{pc}. In each series, 13 different loading speed levels were applied. The test programme is summarized in Table 1.

Table 1. Test programme

σ_{pc} [MPa]	Series	Loading speed [mm/min]												
		0.25	0.5	1	3	5	7	10	13	15	20	30	40	50
0.20	T1	T1_1	T1_2	T1_3	T1_4	T1_5	T1_6	T1-7	T1_8	T1_9	T1_10	T1_11	T1_12	T1_13
0.40	T2	T2_1	T2_2	T2_3	T2_4	T2_5	T2_6	T2_7	T2_8	T2_9	T2_10	T2_11	T2_12	T2_13
0.60	T3	T3_1	T3_2	T3_3	T3_4	T3_5	T3_6	T3_7	T3_8	T3_9	T3_10	T3_11	T3_12	T3_13

3.2. Test set-up, testing procedure and measurements

The test set-up, which was based on the European Standard EN 1052-3 [28], is shown in Fig. 5. After the prescribed curing time, each specimen was placed in the universal testing machine between two load transmission elements and centred to diminish the influence of bending. A hydraulic jack together with the pendulum manometer was used to apply the pre-compression load and maintain it at the constant level during testing. Subsequently, the specimen was subjected to the monotonic shear load by applying a computer-controlled relative displacement (slip) between the middle and one of the outer blocks. The loading speed was kept at a constant level during each test. After reaching the slip value of 0.3 mm in each test, the computer-controlled slip was stopped and kept constant until the shear load was relaxed, i.e. until there was no more change in value of the measured shear load. Then, the specimen was reloaded until the maximum shear load was reached, when the computer-controlled slip was stopped again and kept constant until the shear load relaxed. Finally, the specimen was unloaded and prepared for the next test with the higher loading speed level.

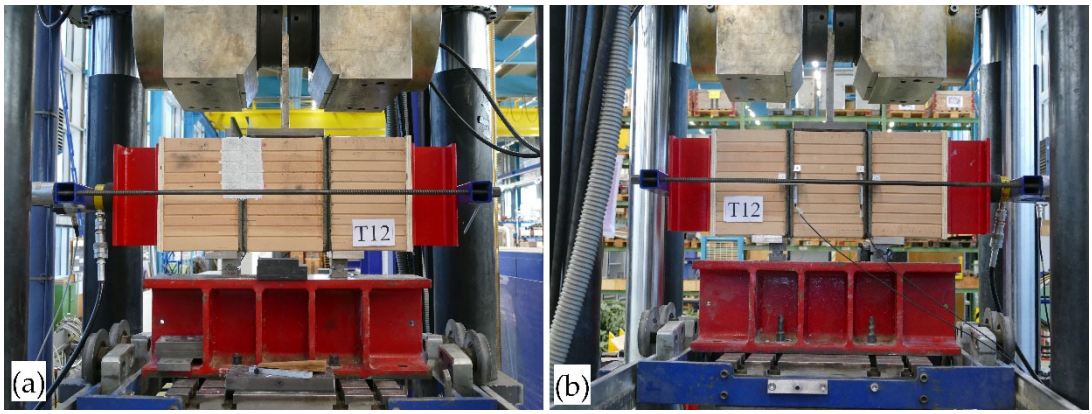

Fig. 5. Test set-up: a) South specimen's side; b) North specimen's side

During the tests, the vertical shear load, the slip between the middle and the outer blocks, and the pre-compression force were recorded. A pair of load cells were used to control the level of the applied pre-compression force, see Fig. 6a. Relative displacement (slip) between the middle and outer blocks were measured by means of two LVDTs on the North side of the specimen. One of the LVDTs was used for the purpose of test control. The LVDTs had a measuring span of 10 mm and rested on L-shape aluminium plates, which in turn were glued to the blocks, see Fig. 6b.

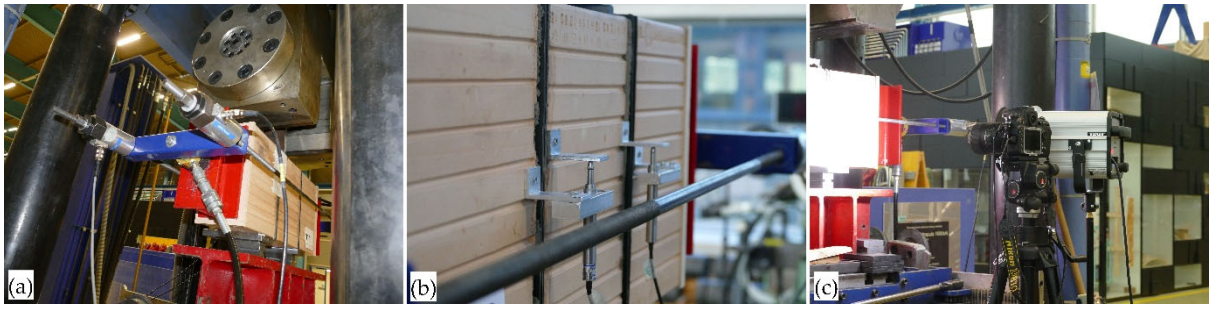

Fig. 6. Measuring devices: a) loading cells; b) LVDTs; c) DIC system

A 2D digital image correlation (DIC) measurement system was applied to gather the information on the displacement field on the surface of a multi-layer bed joint on the South side of the specimen, see Fig. 6c. Detailed description of the used DIC measurement system can be found in [29]. The computer used for data acquisition triggered the DIC camera every 5 seconds. Fig. 7 shows exemplarily the minor principal strain field and shear strain field of specimen T1_1, evaluated at maximum pre-compression load and a slip value of 0.3 mm.

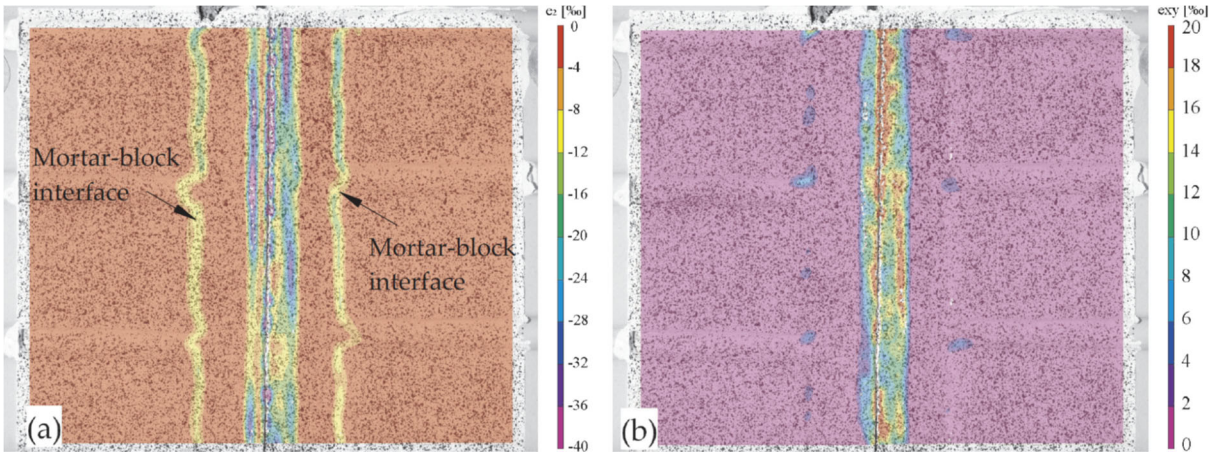

Fig. 7. Specimen T1_1: a) minor principal strain field; b) shear strain field

3.3 Test results and specimen behaviour

Typical shear deformation, i.e. sliding in the multi-layer bed joints was observed in each test, see Fig. 8. Sliding planes formed along the interface between a rubber granulate core soft layer and the protective elastomer layers. For all tests specimens the shear failure did not occur within the units themselves, and no damage to the clay blocks was observed.

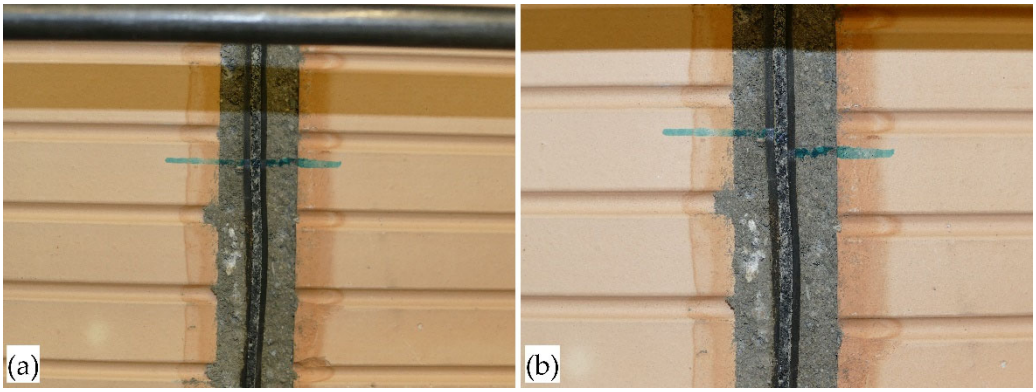

Fig. 8. Multi-layer bed joint: a) before deformation; b) after deformation

Values of the maximum measured shear force per bed joint, H_{max}, are presented in Table 2. This table also reports the values of the shear force after a relaxation, H_{rel}, recorded after the maximum shear force was reached, following the test protocol.

Table 2. Maximal and residual shear forces (values given in kN)

Series		Loading speed [mm/min]												
		0.25	0.5	1	3	5	7	10	13	15	20	30	40	50
T1	H_{max}	3.17	3.04	3.10	3.33	3.30	3.14	3.65	5.18	5.50	5.76	6.21	6.72	6.94
	H_{rel}	2.19	1.92	1.89	1.85	1.81	1.76	1.85	1.79	1.69	1.63	1.63	1.63	1.53
T2	H_{max}	4.22	4.93	5.51	7.01	7.77	8.48	8.86	9.47	9.70	9.99	10.82	10.98	11.68
	H_{rel}	2.75	3.04	2.94	3.13	3.2	3.49	3.39	3.39	3.46	3.29	3.24	2.94	3.23
T3	H_{max}	5.50	6.34	6.82	8.80	10.21	10.66	11.68	12.13	-	13.18	14.40	14.91	15.10
	H_{rel}	3.4	3.4	3.6	3.68	3.74	3.68	3.65	3.58	-	3.68	3.58	3.45	3.36

Typical shear force-slip relationships obtained from the tests are shown in Fig. 9. The deformation value shown in the diagram is the computer-controlled relative displacement (slip) between the middle and outer block. All specimens exhibited a non-linear behaviour almost from the beginning. After reaching the maximum value of the shear force, which in turn depended on the loading speed as well on the pre-compression level, the large majority of specimens developed a plastic plateau.

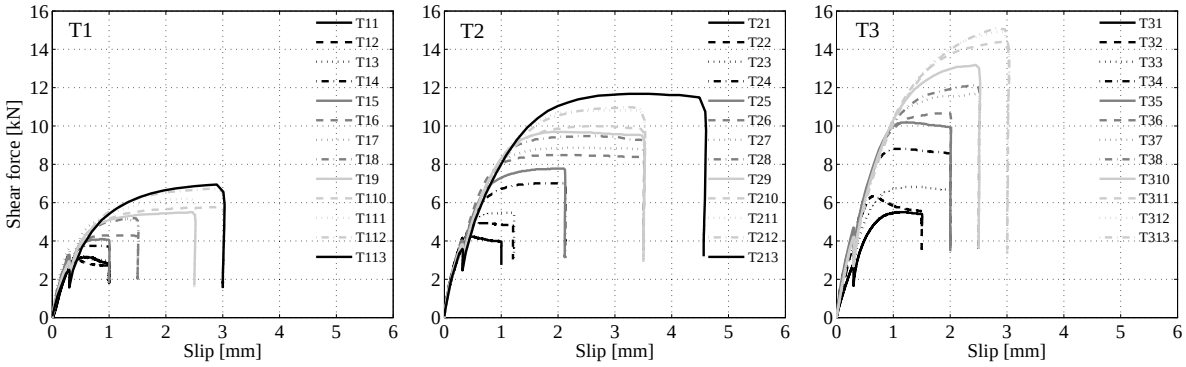

Fig. 9. Measured shear force-slip relationships

Observing the measured shear force-slip relationships given in Fig. 9 for each pre-compression separately, one notices that all specimens exhibited a rather similar (initial) response up to a certain level of shear force, i.e. of slip, which did not depend on the loading speed. Thereafter, load-deformation curves differ from one another. Specimens developed larger shear resistance with increasing loading speed, cf. Table 2. A slight inconsistency can be noticed in measured values of maximum shear force for the first six specimens of series T1. This is caused by the sensitivity of the system used to keep the pre-compression load at the constant level, which was especially demanding during testing of the specimens of series T1 - due to the low pre-compression level of 0.20 MPa. Values of shear force after the relaxation, which indicate the force limit of the elastic behaviour, are reported in Table 2. Since the calculated values of coefficient of variation from the sample of shear force after the relaxation measured in test series T1, T2 and T3 are 9.5%, 7% and 3.5%, respectively, it can be concluded that the influence of the loading speed on the H_{rel} is small and can be neglected. When comparing the response characteristics from corresponding specimens of different test series, it can be seen that the values of maximum shear force, shear force after the relaxation and the initial stiffness increase with increasing pre-compression, cf. Table 2 and Fig. 9. Given the above, it may be concluded that the model assumption for the linear elastic-perfectly viscoplastic behaviour of the multi-layer bed joint is justified.

4. Model parameters and discussion

In order to define the shear stress dependence on the loading speed and the displacement (slip) one needs four parameters, i.e. τ_y, G_{ml}, ζ, and Δt_{ml}, cf. Section 2. Firstly, using the results from monotonic tests presented in Section 3, G_{ml} and Δt_{ml} will be determined. Secondly, from the results of relaxation tests (also described in Section 3) τ_y will follow. Finally, from static-cyclic tests described in [14] the parameter ζ will be determined.

The test results presented in the previous section allow one to determine two parameters that describe the deformation of the multi-layer bed joint when subjected to the shear and the pre-compression load. Firstly, values of the contraction of the thickness of the multi-layer bed joint Δt_{ml} were measured (using DIC) during application the pre-compression load. The values, which correspond to the applied levels of pre-compression, are given in Table 3. Secondly, using the values of relative displacement (slip) measured within the initial phase of the application of the shear load, i.e. before sliding, where one can assume that the soft layers of the multi-layer bed joint remain connected to each other and deform in pure shear, and that the shear deformation of the mortar layers is relatively small and therefore negligible, the values of the multi-layer bed joint shear modulus, G_{ml}, can be determined using following equation:

$$G_{ml} = \frac{H \cdot \left(t_{ml} - \Delta t_{ml}\right)}{A_b \cdot d} \tag{14}$$

Eq. (14) is derived from Eq. (2) considering that $\tau = H/A_b$, where H is the instantaneous shear force and A_b is the gross cross-section area of the block used, the multi-layer bed joint represents a localized zone of intense shearing with constant thickness t_{ml}-Δt_{ml} and that the relationship between the shear strain and the slip in the multi-layer bed joint is $\gamma (t_{ml}$-$\Delta t_{ml}) = d$, see Eq. (12). The values of the multi-layer bed joint shear modulus calculated for a slip value of 0.1 mm are given in Table 3.

As expected, the larger contractions of the multi-layer bed joint were measured for the larger pre-compression level. However, the pre-compression did not influence the value of shear modulus of the multi-layer bed joint, which on average equalled 2.0 MPa. As already mentioned, the specimens in each series had rather identical (initial) response, i.e. initial stiffness, up to a certain level of shear

force. Since the initial stiffness is governed by the value of G_{ml}, it may be concluded that the loading speed did not affect G_{ml}.

Table 3. Contraction and shear modulus of the multi-layer bed joint

Series	σ_{pc} [MPa]	Δt_{ml} [mm]	G_{ml} [MPa]
T1	0.20	0.24	2.00
T2	0.40	0.27	1.95
T3	0.60	0.53	2.20

In order to assess the third parameter τ_y, the controlled bed joint slip was stopped after reaching the maximum shear force in each test and the relaxation of the shear load was recorded. The relaxation lasted until the (bed joint) shear force became constant, giving the value of H_{rel}, i.e. $\tau_y=H_{rel}/A_b$. The results show that the value of τ_y depends on the level of pre-compression, but that it is independent of the shear loading speed, cf. Table 2 for values of the shear force after the relaxation. With known thickness of multi-layer bed joint (t_{ml}=7.4 mm excluding the mortar layers) and values of τ_y, G_{ml} and Δt_{ml}, the corresponding slip at the elastic limit, d_y, can be calculated using Eq. (15), see Table 4.

$$d_y = \frac{\tau_y \cdot \left(t_{ml} - \Delta t_{ml}\right)}{G_{ml}} \tag{15}$$

Table 4. Elastic limit determination

Test series	Pre-compression [MPa]	[a] τ_y [MPa]	G_{ml} [MPa]	d_y [mm]
T1	0.20	0.04	2.00	0.15
T2	0.40	0.07	2.00	0.25
T3	0.60	0.08	2.00	0.28

[a]Average from the sample of calculated values of τ_y for different loading speeds

The remaining (viscosity) parameter ζ could be obtained by calibrating the model so that it matches the shear resistances measured from the monotonic shear tests presented in Section 3. However, since the model should account for the elastic (initial) shear stiffness degradation caused by cyclic loading, the data on the shear capacity obtained from the series of static-cyclic shear tests on masonry triplets

with multi-layer bed joints, [14], will be used. Note that only the specimens with a rubber granulate core soft layer will be considered, i.e. the G series. Test data are available for three levels of pre-compression (each level with two replicates), namely 0.2 MPa, 0.6 MPa and 1.0 MPa, with a loading speed range of 0.5-10 mm/min. Assuming that the values of d_y, G_{ml} and Δt_{ml} are the same as estimated for the monotonic test series, the corresponding values of τ_y can be calculated for different levels of pre-compression by using Eq. (15), see Table 5 for results.

Table 5. Elastic limit determined from static-cyclic tests [14]

Test	Pre-compression [MPa]	d_y [mm]	G_{ml} [MPa]	τ_y [MPa]
G1_1 and G1_2	0.20	0.15	2.00	0.04
G2_1 and G2_2	0.60	0.28	2.00	0.08
G3_1 and G3_2	1.00	[a]0.35	2.00	0.18

[a]Value obtained by extrapolating the measured data from Table 4

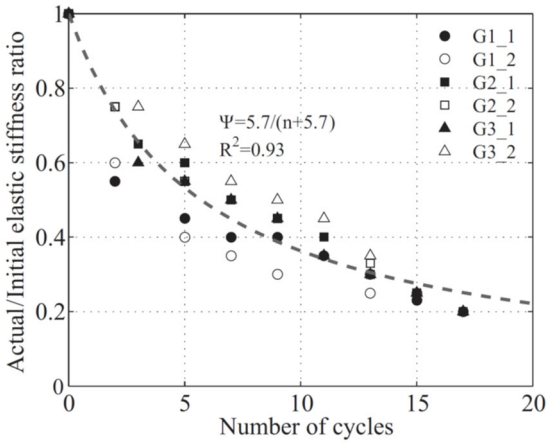

Fig. 10. Relative degradation of the elastic stiffness vs. the number of performed loading cycles

In order to account for the elastic (initial) stiffness degradation, a coefficient ψ is introduced. This coefficient depends on the number of loading cycles performed, n, and will be used as a multiplier of the shear modulus G_{ml}. The data from the static-cyclic shear tests indicate that the evolution of the (relative) degradation of the elastic stiffness, measured at the beginning of each first pushing semi-cycle applied, is independent of the level of pre-compression and that it can be described using a rational function, see Fig. 10. Thus, the elastic (initial) stiffness degradation dependent on the number

of loading cycles can be accounted for by multiplying the shear modulus by a coefficient, namely $\psi = 5.7/(n+5.7)$, cf. Fig. 10.

Now applying the coefficient ψ, one obtains analogue to Eq. (13), with $\tau = H/A_b$, the following relationship between the shear force H and slip d:

$$H = H_y \cdot \left[1 + \frac{\dot{d}}{t_{ml} - \Delta t_{ml}} \cdot \zeta \cdot \left(1 - e^{-\frac{\psi \cdot G_{ml} \cdot A_b}{H_y \cdot \zeta} \cdot \frac{d - d_y}{\dot{d}}} \right) \right]. \tag{16}$$

Finally, with defined (initial) values of τ_y and d_y and considering the degradation of the elastic stiffness, the model can be calibrated for the parameter ζ, so that it reaches the same values of the maximum shear force measured for each first pushing semi-cycle applied during the static-cyclic tests on masonry triplets from [14]. Thereby the loading speed is considered as constant (and equal to the average value) during each cycle in spite of the sinusoidal loading pattern that implies a variable loading speed during the cycle, see [14]. Values of the model parameter ζ are calculated for each level of pre-compression and for each replicate, except for the replicate G3_1, whose resistance was far below that expected, and is thus excluded from the analysis. It should be also noted that values of τ_y are kept constant, while the values of d_y change as the elastic (initial) stiffness degrades with the increase of the number of loading cycles. The results obtained, as well the input values for model calibration, are presented in Table 6. Fig. 11 shows the dependency of the parameter ζ on the loading speed together with the corresponding regression curves.

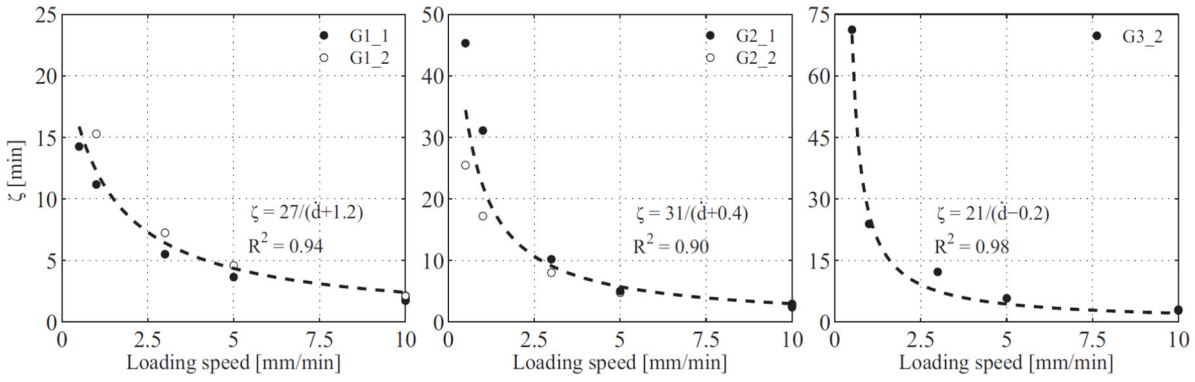

Fig. 11. Dependency of the parameter ζ on the loading speed

346 Table 6. Input values for model calibration [14] and the obtained values for parameter ζ

Specimen	Parameter	Loading step						
G1_1	Max shear force [kN]	2.51	3.21	4.14	4.45	4.58	4.34	4.30
	Max slip [mm]	1.98	2.98	4.89	9.63	14.42	19.21	28.58
	Loading speed [mm/min]	0.5	1	3	5	10	10	10
	ζ [min]	14.26	11.18	5.5	3.64	1.89	1.76	1.73
G1_2	Max shear force [kN]	2.19	3.89	5.00	5.28	4.97	4.94	-
	Max slip [mm]	0.87	2.66	4.49	9.20	18.64	26.83	-
	Loading speed [mm/min]	0.5	1	3	5	10	10	-
	ζ [min]	10.77	15.28	7.23	4.59	2.12	2.1	-
G2_1	Max shear force [kN]	5.83	7.14	9.32	10.48	12.11	11.98	10.69
	Max slip [mm]	1.52	2.26	4.14	8.87	13.44	18.11	30.00
	Loading speed [mm/min]	0.5	1	3	5	10	10	10
	ζ [min]	45.29	31.11	10.21	5.03	2.94	2.83	2.41
G2_2	Max shear force [kN]	5.74	6.98	9.02	10.18	11.82	11.59	-
	Max slip [mm]	1.89	2.91	4.76	9.48	14.25	19.06	-
	Loading speed [mm/min]	0.5	1	3	5	10	10	-
	ζ [min]	25.47	17.22	8.01	4.73	2.81	2.69	-
G3_2	Max shear force [kN]	5.79	10.07	13.76	15.63	17.51	16.63	-
	Max slip [mm]	0.89	2.81	4.69	9.48	19.01	28.19	-
	Loading speed [mm/min]	0.5	1	3	5	10	10	-
	ζ [min]	71.22	23.88	12.24	5.79	3.02	2.78	-

5. Conclusions and outlook

The structural behaviour of the multi-layer bed joint subjected to cyclic shear was described using a mechanical model consisting of an elastic spring mounted in series with a dashpot and a frictional slider. The mechanical model is characterized by three material parameters, which could be assessed from various series of monotonic and static-cyclic tests on small specimens (triplets). The model is capable of capturing of the loading-speed dependent in-plane shear load-slip behaviour, which is thus assumed to be linear elastic-perfectly viscoplastic. Although the model parameters are determined for the multi-layer bed joint with a rubber granulate core soft layer, the parameter space can be extended to other types of core soft layer once the appropriate test data becomes available.

The next step in this research is modelling of full-scale unreinforced masonry walls with a multi-layer bed joint. The current joint model is being extended in order to be able to describe the in-plane horizontal force-displacement behaviour of URM walls with the multi-layer bed joint at the bottom of the wall. The results from our own tests on URM walls with a multi-layer bottom bed joint [15] will be used for the model validation.

6. Acknowledgements

The funding from the Swiss National Science Foundation (Grant 200020_169119) as well as the support from HBT-ISOL AG, who supplied the soft layers free of charge and the assistance of Mr. Felix Walker from ZZ Wancor AG in preparing the specimens, are gratefully acknowledged.

REFERENCES

[1] Suter GT, Ibrahim KS. Shear resistance of damp-proof-course materials in brick-mortar joints. In: Proceedings of the 6th Canadian Masonry Symposium, Saskatoon; 1992. p. 119-30.

[2] Zhuge Y, Mills J. The behaviour of masonry walls containing a damp proof course under cyclic loads. In: Proceedings of the 2nd Australasian Structural Engineering Conference, Auckland; 1998. p. 655-61.

[3] Griffith MC, Page AW. On the seismic capacity of typical DPC and slip joints in unreinforced masonry buildings. Australian J Struct Eng 1998;1(2):133-40.

[4] Simundic G, Page AW, Chen Q. The cyclic and long term behaviour of slip joints in load-bearing masonry construction. In: Proceedings of the 12th International Brick/Block Masonry Conference, Madrid; 2000. p. 1409-20.

[5] Trajkovski S, Totoev Y. Shear strength of masonry including damp proof course: experimental determination at different strain rates. In: Proceedings of the 6th International Masonry Symposium, London; 2002. p. 487-92.

[6] Totoev Y, Simundic G. New test for the shear transfer capacity of horizontal slip joints in load-bearing masonry. In: Proceedings of the 10th Canadian Masonry Symposium, Banff; 2005. p. 863-72.

[7] Mojsilović N. Masonry elements with damp-proof course membrane: Assessment of shear strength parameters. Constr Build Mater 2012;35:1002-12.

[8] Mojsilović N, Simundic G, Page AW. Static-Cyclic Shear Tests on Masonry Triplets with a Damp-Proof Course Membrane. In: Proceedings of the 12th Canadian Masonry Symposium, Vancouver; 2013. Paper No. 159.

[9] Mojsilović N, Simundic G, Page AW. Static-cyclic shear tests on masonry wallettes with a damp-proof course membrane. Report no. 319. Institute of Structural Engineering, ETH Zurich; 2009. pp. 82.

[10] Mojsilović N, Simundic G, Page AW. Masonry wallettes with damp-proof course membrane subjected to cyclic shear: An experimental study. Constr Build Mater 2010;24 (11):2135-44.

[11] Mojsilović N, Stojadinović B, Barandun A, Vögeli C. Seismic behaviour of masonry walls with soft-layer wall bearings. In: Proceedings of the 5th International Conference on Structural Engineering, Mechanics and Computation, Cape Town; 2013. p. 1865-70.

[12] Vögeli C, Mojsilović N, Stojadinović B. Masonry wallettes with a soft layer bed joint: Behaviour under static-cyclic loading, Eng Struct 2015;86:16-32.

[13] M. Petrović, B. Stojadinović, N. Mojsilović, I-Shaped Unreinforced Masonry Wallettes with a Soft-Layer Bed Joint: Behavior under Static-Cyclic Shear, J. Struct. Eng. 143 (11) (2017) 04017154. doi:10.1061/(ASCE)ST.1943-541X.0001884.

[14] N. Mojsilović, M. Petrović, X.R. Anglada, Masonry elements with multi-layer bed joints: Behaviour under monotonic and static-cyclic shear, Constr. Build. Mater. 100 (2015) 149-162. doi:10.1016/j.conbuildmat.2015.09.065.

[15] M. Petrović, N. Mojsilović, B. Stojadinović, Masonry walls with a multi-layer bed joint subjected to in-plane cyclic loading: An experimental investigation, Eng. Struct. 143 (2017) 189-203. doi:10.1016/j.engstruct.2017.04.025.

[16] Persson BNJ. Sliding friction: Physical principles and applications. 2nd ed. Berlin: Springer; 2000.

[17] Popov VL, Hess M. Method of dimensionality reduction in contact mechanics and friction. Berlin: Springer; 2015.

[18] Richardson RSH, Nolle H. Surface friction under time-dependent loads. Wear. 1976;37,87-101.

[19] Persson BNJ, Albohr O, Mancosu F, Peveri V, Samoilov VN, Sivebaek IM. On the nature of the static friction, kinetic friction and creep. Wear. 2003;254,835-51.

[20] Li Q, Dimaki A, Popov M, Psakhie SG, Popov VL. Kinetics of the coefficient of friction of elastomers. Sci. Rep. 2014;4:5795. DOI: 10.1038/srep05795.

[21] Nettingsmeier J, Wriggers P. Frictional contact of elastomer materials on rough rigid surfaces. Proc. Applied Mathematics and Mechanics (PAMM). 2004;4:360–1.

[22] Ibrahimbegović A. Nonlinear solid mechanics, Berlin: Springer; 2009.

[23] E.A. de Souza Neto, D. Perić, D.R.J. Owen, Computational methods for plasticity: theory and applications, John Wiley & Sons, Chichester, UK, 2008.

[24] P.W. Oberender, A.M. Puzrin, Observation-guided constitutive modelling for creeping landslides, Géotechnique 66 (2016) 232–247. doi:10.1680/jgeot.15.LM.003.

[25] Petrović M. Use of soft layers for seismic response modification of structural masonry walls. PhD Thesis, ETH Zurich, 2018.

[26] EN 772-1, Methods of test for masonry units - Part 1: Determination of compressive strength, European Committee for Standardization, Brussels, 2000.

[27] EN 1015-11:1999. Methods of test for mortar for masonry – Part 11: Determination of flexural and compressive strength of hardened mortar. European committee for standardization, Brussels; 1999.

[28] EN 1052-3:2002. Methods of test for masonry – Part 3: Determination of initial shear strength. European committee for standardization, Brussels; 2002.

[29] N. Mojsilović, A.H. Salmanpour, Masonry walls subjected to in-plane cyclic loading: application of digital image correlation for deformation field measurement, Int. J. Mason. Res. Innov. 1 (2016) 165-187. doi:10.1504/IJMRI.2016.077473.